Translating Multiscale Cancer Models into Clinical Trials: Simulating Breast Cancer Tumor Dynamics within the Framework of the "Trial of Principle" Clinical Trial and the ACGT Project.

Eleni A. Kolokotroni, Georgios S. Stamatakos, Dimitra D. Dionysiou, Eleni Ch. Georgiadi,
Christine Desmedt, Norbert M. Graf

Abstract— The potential of cancer multilevel modeling has been particularly emphasized over the past years. Integration of multiscale experimental and clinical information pertaining to cancer via advanced computer models seems to considerably accelerate optimization of cancer treatment in the patient individualized context. However, a *sine qua non* prerequisite for such models to reach clinical practice is to be thoroughly tested through clinical trials for validation and optimization purposes. This is one of the major goals of the European Commission funded "Advancing Clinico-Genomic Trials on Cancer" (ACGT) project. This paper presents a discrete state based, four dimensional, multiscale tumor dynamics model that has been specially developed by the *In Silico* Oncology Group in order to mimic the Trial Of Principle (TOP) clinical trial concerning breast cancer treated with epirubicin. The TOP trial constitutes one of the ACGT clinical trials. A substantial part of the model can address other tumor types as well. The actual pseudoanonymized imaging, histopathological, molecular and clinical data of the patient are exploited. Special emphasis is put on the effect of cancer stem/clonogenic, progenitor, differentiated and dead cells, the cell category transition rates and the cell category relative populations within the tumor from the treatment baseline onwards. The importance of adaptation of the cell category relative populations to the cell category transition rates for free tumor growth is revealed and the concept of a pertinent nomogram is introduced. A method which ensures adaptation of these two sets of entities at the beginning of the simulation execution is proposed and subsequently successfully applied. Convergence and code checking issues are addressed. Indicative parametric/sensitivity studies are presented along with specific numerical findings. The model's behavior substantiates its potential to serve as the basis of a treatment optimization system following an eventually succesful completion of the clinical validation and optimization process.

I. INTRODUCTION

WOLDWIDE, breast cancer is the second most commonly diagnosed cancer (both sexes counted) and the fifth most common cause of cancer death [1]. The current trend in the treatment of localized breast carcinoma is the combination of neoadjuvant chemotherapy (preoperative therapy given as initial treatment) and surgery with adjuvant therapy. The preoperative systematic therapy contributes to the shrinkage of the tumor and the surgery required area, even the avoidance of mastectomy in some cases [2]. The chemotherapy agent and the therapeutic scheme chosen are based on the experience from clinical practice. However, due to the heterogeneity of the disease, the effectiveness and the benefits of the adopted therapy vary from individual to individual. Computer modeling and simulation are expected to considerably support treatment optimization in the patient's individualized context.

In this context a number of computational models of solid tumor response to chemotherapy that might in principle be applicable to breast cancer have been developed. The following represent only a few examples. Chuang [3] presented a theoretical study concerning the applicability of certain early pharmacokinetic and cell kinetic models for cancer chemotherapeutic systems. Ozawa et al.[4] presented a pharmacodynamic model for the cell cycle phase-specific antitumor agents as well as for the cell cycle phase-nonspecific agents. Gardner [5] developed a computer model, the kinetically tailored treatment or KITT model, to predict drug combinations, doses, and schedules likely to be effective in reducing tumor size and prolonging patient's life.

In this paper a novel spatiotemporal, patient specific, discrete state simulation model of solid tumor response to chemotherapeutic treatment *in vivo* is delineated. Monte Carlo and continuous mathematics are also used although to

E. A. Kolokotroni is with the National Technical University of Athens, Institute of Communication and Computer Systems, *In Silico* Oncology Group, Iroon Polytechniou 9, Zografos, GR-157 80, Greece (e-mail: ekolok@iccs.gr).

G. S. Stamatakos (corresponding author) is with the National Technical University of Athens, Institute of Communications and Computer Systems, *In Silico* Oncology Group, Iroon Polytechniou 9, Zografos, GR-157 80, Greece (phone: + 30 210 772 2288, fax: + 30 210 772 3557, e-mail: gestam@central.ntua.gr).

D. D. Dionysiou is with the National Technical University of Athens, Institute of Communications and Computer Systems, *In Silico* Oncology Group, Iroon Polytechniou 9, Zografos, GR-157 80, Greece (e-mail: dimdio@esd.ece.ntua.gr).

E. Ch. Georgiadi is with the National Technical University of Athens, Institute of Communication and Computer Systems, *In Silico* Oncology Group, Iroon Polytechniou 9, Zografos, GR-157 80, Greece (e-mail: egeorg@ics.forth.gr)and the Foundation for Research and Technology – Hellas, Institute of Computer Science, Biomedical Informatics Laboratory, N. Plastira 100, Vassilika Vouton, GR-700 13 Heraklion, Crete, Greece

C.Desmedt is with the Institut Jules Bordet - Centre des Tumeurs, rue Héger Bordet 1, 1000 Bruxelles, Belgium (e-mail : christine.desmedt@bordet.be)

N.Graf is with the University Hospital of the Saarland, Paediatric Haematology and Oncology, D-66421 Homburg,, Germany (e-mail: norbert.Graf@uniklinikum-saarland.de).

a lesser extent. Even though the case of breast cancer is addressed, parts of the model can be easily adapted to other types of solid tumor. Several numerical aspects of the model reflecting actual biological mechanisms are revealed and appropriately treated.

II. THE TOP TRIAL

The chemotherapeutically treated breast cancer tumor, considered in the present work is mimicking a branch of the clinical study known as *Trial of Principle* (TOP) [6]. This study aims to evaluate the topoisomerase II alpha gene amplification and protein overexpression as markers predicting the efficacy of epirubicin in the primary treatment of breast cancer patients. The trial addresses non-metastatic, early breast cancer patients with ER-negative tumors of size >2cm as defined by ultrasound. The patients are treated with four cycles of single-agent epirubicin ($100mg/m^2$, q3weeks) as neoadjuvant treatment, followed by surgery and adjuvant chemotherapy [6].

III. A BRIEF OUTLINE OF THE MODEL

A. The Model Basics

A number of core algorithms of the model originate from work previously published by the *In Silico* Oncology Group (www.in-silico-oncology.iccs.ntua.gr) such as [7-10] although considerable extensions and improvements have been made. Novel algorithms concerning several further aspects of the *natural phenomenon* under consideration such as the simulation of the cancer progenitor or limited mitotic potential (limp) cell dynamics, the achievement of adaptation of the cell category relative populations to the transition rates among the various cell categories for free tumor growth (in this more complex setting), model compatible epirubicin pharmacokinetics modeling etc. have been developed, implemented, checked and numerically studied.

In this paper a spatially homogeneous tumor of spherical shape is considered. This is a first approximation based on accumulated clinical experience regarding the shape of breast cancer tumors and on the fact that the tumor size as reported in the Case Report Forms (CRFs) of the TOP trial is defined as the maximum diameter measured by ultrasound imaging. More general shapes and non metabolically homogeneous tumor structures will be addressed in a subsequent version. Approaches such as the ones already developed by our group and presented in [7-10] will be recruited to tackle this aspect. in the following a brief aoutline of the model will be attempted.

A cubic discretizing mesh is superimposed upon the anatomic region of interest and is scanned every hour in order to allow the local application of basic biological rules and subsequently lead to the spatiotemporal simulation of the evolution of the tumor system. The elementary cube of the mesh is called *geometrical cell* (GC) and in this paper corresponds to a volume of $1mm^3$. Each geometrical cell

belonging to the tumor is considered to initially accomodate 10^6 biological cells. This corrseponds to the typical cell density of 10^6 cells/mm^3 being the standard assumption particularly in radiobiological models [11]). Conservation of this (mean) cell density throughout the simulation is one of the tasks of the code. An hourly scan consists of four constituent scans. The first one primarily deals with the simulation of the cell cycle. The second one deals with the eventual unloading of each overloaded geometrical cell due to the occurence of cell mitoses. It also handles the eventual creation of one or more new GCs that will be occupied by the tumor thus leading to a differential tumor expansion. The third one deals with the re-establishment of the normal cell density by freeing geometrical cells containing too few biological cells and therefore leading to a differential tumor shrinkage. The fourth one deals with the restauration of tumor contiguity in case that tumor fragmentation has taken place. Random directions covering the entire angular space for differential tumor expansion and shrinkage are used.

TABLE I
INPUT PARAMETERS AND THEIR ASSIGNED VALUES CORRESPONDING TO THE RESULTS PRESENTED IN THIS PAPER UNLESS OTHERWISE STATED

Symbol	Description	Value
T_c	Cell cycle duration	60h *
T_{G1}	Duration of Gap 1 phase	$0.41(T_c - T_M)$
T_S	Duration of DNA synthesis phase	$0.41(T_c - T_M)$
T_{G2}	Duration of Gap 2 phase	$0.18(T_c - T_M)$
T_M	Duration of mitosis phase	1h
T_{G0}	Duration of dormant phase	96h
T_N	Time period needed for necrosis' products to disappear from the tumour	20h
T_A	Time duration needed for apoptosis products to be removed from the tumour	6h
N_{LIMP}	Number of mitosis performed by progenitor cells before they become differentiated	3
R_A	Apoptosis rate of cancer cells	0.001
R_{NDiff}	Necrotic rate of differentiated cells	0.001
R_{ADiff}	Apoptosis rate of differentiated cells	0.001
P_{G0toG1}	Fraction of dormant cells that re-enter cell cycle	0.01
P_{MtoG0}	Fraction of cells that enter G0 phase following mitosis	0.1
P_{sym}	Fraction of stem cells that perform symmetric division	0.18

*Based on literature, breast cancer cell cycle duration can vary from 23h to 90h. An intermediate value of 60h is considered here. Cell cycle phase relative durations are based in [12] and further related literature. Rates and fraction values have been assumed based on both qualitative or semiquantitative information and logic. Extensive use of series of TOP clinical trial data are expected to allow more quantitatively refined assumptions.

One of the central features of the model is the distinction of proliferating cells in stem and progenitor (limp) cells as well as the consideration of differentiated cells. This approach provides the flexibility to simulate tumors of differing differentiation degree (grade) and address the chemotherapeutic drug effect on the various cell categories (stem-limp) separately. Such a modeling approach is in accordance with the concept that breast cancer originates

from mammary stem cells, a theory that is gaining more and more ground.

Fig. 1 depicts the cytokinetic model proposed and adopted for the case of free tumor growth. An extension of this diagram is used in order to model the chemothepy treated tumor cytokinetics. The following types (categories) of cells can be identified : *stem/clonogenic cells* i.e. cells assumed to possess unlimited proliferative potential, *limp (limited mitotic potential)* or *progenitor cells* i.e. cells with limited mitotic potential (three divisions are assumed before terminal differentiation occurs), *differentiated (diff) cells* i.e. terminally differentiated cells, *necrotic cells* i.e cells that have already died through necrosis and *apoptotic cells* i.e. cells that have already died through apoptosis.
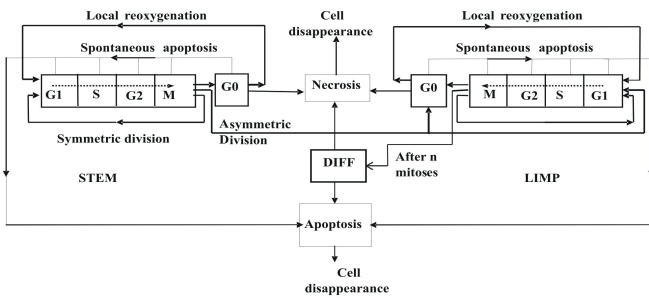
Fig 1. A generic cytokinetic model for free tumor growth. STEM: stem cells. LIMP: Limited proliferative potential cells. DIFF: terminally differentiated cells

A proliferating tumor cell (stem or limp) passes through the phases gap 1 (G1), DNA synthesis (S), gap 2 (G2) and mitosis (M). After completion of mitosis the "daughter" cells may enter the resting (dormant) G0 phase with a fraction (percentage) P_{MtoG0} or (re-) enter the G1 phase depending on the nutrient supply and oxygenation at their current spatial position. A dormant or proliferating cell residing in any phase of the cycle may die due to ageing and spontaneous apoptosis with a rate R_A (probability/hour). A dormant cell is assumed to be able to survive for an interval T_{G0} unless the metabolic conditions (oxygenation, nutrition) in its region are inproved before expiration of T_{G0}. If the local metabolic conditions become adequate it re-enters the G1 phase. Otherwise it enters the necrotic phase after T_{G0}. The differentiated cells may die due to apoptosis or necrosis each one expressed by a different rate.

Each stem cell can undergo either a *symmetric* or an *asymmetric* division. The occurence of a symmetric division (giving birth to two stem cells) is quantified by the rate (percentage) parameter P_{sym}. Asymmetic division gives birth to one stem and one progenitor cell. Table I summarizes the input parameters of the code and the values corresponding to the results presented in the present work unless otherwise stated.

B. Epirubicin Pharmakokinetics

Epirubicin pharmacokinetics has been described in various studies by an open three-compartment model with elimination from the central compartment [13]. The pharmacokinetics module of the model [see Appendix A] enables the calculation of the area under curve (AUC) from the inter-compartmental rate constants for any given drug dose and volume of distribution. Typical values for the volume of distribution (V_d) and clearance (CL) have been derived from [13]. Based on these values the elimination constant can be calculated from (1) and substituted into the tri-phasic model equations.

$$k_{el} = \frac{CL}{V_d} \quad (1)$$

For the determination of the transfer rate constants the SAAM II software tool developed at the University of Washington has been used [14]. The specific values of V_d, CL and dose in conjunction with the experimental data of plasma concentration versus time have been exploited in order to determine the three compartment model parameter values through a fitting process. This has led to the estimation of the transfer rate constants (Table II). Subsequently the AUC can be estimated for several doses.

TABLE II
TYPICAL PARAMETER VALUES ASSIGNED TO THE MODEL MODULE DEALING WITH EPIRUBICIN PHARMACOKINETICS AND PHARMACODYNAMICS

Symbol	Parameter	Value
D	Dose	100 mg/m^2
V_d	Volume of distribution	480.1L/m^2
k_{12}	Inter-compartmental transfer rate constant	0.1498
k_{21}	Inter-compartmental transfer rate constant	0.7231
k_{13}	Inter-compartmental transfer rate constant	0.1498
k_{31}	Inter-compartmental transfer rate constant	0.7231
k_{el}	Elimination rate constant	0.155h^{-1}
AUC	Area Under Curve	2/3*0.8877mg*h/L≈ 0.592mg*h/L
SF	Survival fraction	≈ 0.65

C. Epirbicin Pharmacodynamics

Epirubicin is an anthracycline chemotherapeutic agent, derivative of doxorubicin. It exerts its cytotoxic action through various mechanisms; the most established one is intercalation between bases of double stranded DNA thereby inhibiting DNA synthesis and function. It interferes with DNA transcription and inhibits topoisomerase II by forming a complex with DNA and topoisomerase II, which leads to DNA strand breaks. It also acts to form toxic oxygen-free radicals, causing DNA strand breaks, and inhibiting DNA synthesis and function [15]. Epirubicin is considered a cell cycle non-specific drug [12].

In the simulation model tumor cells are assumed to absorb

the drug at all cycling phases and apoptotic death occurs at the end of the S phase. In specific cases epirubicin is favored over other anthracycline drugs (doxorubicin) as it appears to cause fewer side-effects due to its less toxic nature at equivalent therapeutic doses.
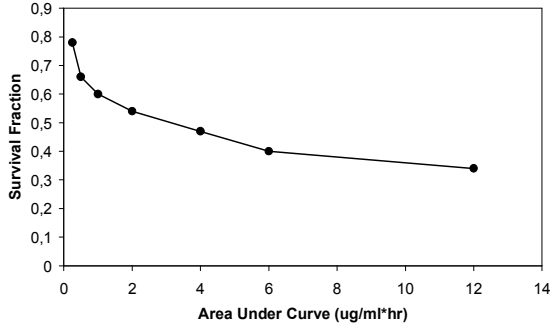
Fig. 2. Experimental data for HeLa cells survival as a function of epirubicin AUC.

As a first approximation, the survival fraction of epirubicin treated tumor cells is calculated using experimental data concerning the pharmacodynamics of epirubicin. More specifically the *in vitro* cytotoxicity of epirubicin on HeLa cells which is available through the Food and Drug Administration [16] as depicted in Fig. 2 has been considered. The survival fraction for any realistic dose for which no experimental data are available is approximately calculated through linear interpolation. Since drug penetration into the tumor is limited due to the imperfections of neovascularization, the previously calculated AUC is multiplied by a factor of 2/3. This is also in agreement with the observation that for human breast cancer tumors steep doxorubicin concentration gradients may appear. [17]. At a subsequent stage the individual patient's gene expression data will be used to perturb the population based mean cell survival fraction. In this way an appropriate molecular signature of the patient will be exploited and therefore further individualizion of the treatment plan will be achieved.

D. The Simulated Chemotherapeutic Scheme

The case of primary chemotherapy ("neo-adjuvant" chemotherapy) with single-agent epirubicin (100 mg/m² i.v. once every 3 weeks for 4 consecutive cycles) for early breast cancer patients, in accordance to the TOP trial is addressed. The simulated tumor is left to grow for 2 weeks before the first drug dose administration takes place. This is assumed to reflect a typical time interval between the point at which diagnostic imaging data are obtained and the initiation of chemotherapy. Any other time interval can be considered as well.
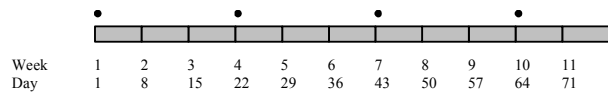
Fig. 3. The dose fractionation considered. Each drug administration session is denoted by a dot.

IV. A PRELIMINARY CHECK OF THE MODEL

If at the beginning of a simulation execution initialization of the population fractions (percentages or relative populations) of the various cell categories (e.g. dormant stem cells, proliferating stem cells, dormant progenitor cells etc) within each geometrical cell of the discretization mesh is arbitrarily made it is very likely to end up with a peculiar and unrealistic free tumor growth behavior. For example there may appear an unexpected (abnormal) decrease of the tumor volume followed by a volume increase. This is due to the lack of adaptation of the cell category transition rates to the initial cell category relative populations. In order to avoid such an unrealistic behavior the concept of the *nomogram* correlating cell category transition rates with cell category relative populations for free tumor growth has been introduced. Fig. 4 shows the number of proliferating and total tumor cells as a function of time for the case of a correct adaptation of the transition rates to the relative populations and the same numbers when there is lack of such adapation (arbitrary selection of initial relative populations in relation to transition rates). In both cases the same transition rates but different initial relative polulation of each cell category (stem, limp, diff and dead cells) have been assumed. It is pointed out that cell category transition rates are considered approximately constant for the relatively small real time interval addressed by a typical simulation. Obviously cell category transition rates are expected to change considerably with time on a much larger time scale (e.g. from the appearance of the first tumor cell to the formation of a clinically detectable tumor).
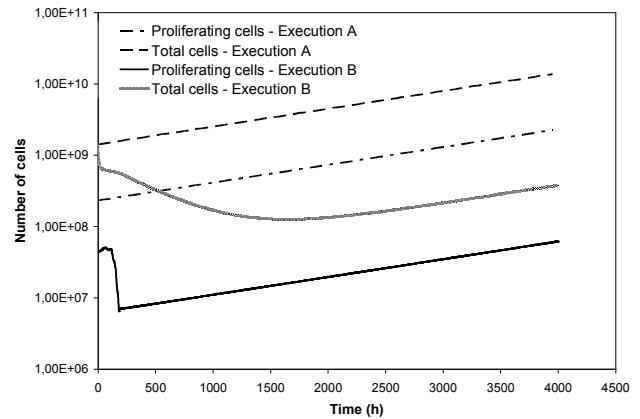
Fig. 4. The effect of arbitrary initialization of the cell category relative populations on tumor growth. Execution A corresponds to a *correct* populations initialization compatible with the cell category transition rates. Cell numbers increase smoothly and monotonically from the beginning of the simulation onwards. Execution B corresponds to an arbitrary population initialization. Cell numbers behave unrealistically (lack of monotonicity). All transition parameters and the cell cycle duration are the same in both cases (Table I). The initial tumor has a diameter of 14 mm.

Subsequently, a number of exploratory simulation executions have been performed in order to match the initial relative populations of the various cell categories with

appropriate cell category transition rates for various cell cycle durations. An example is given in Table III where indicative cell category relative populations (fractions) have been defined for specific values of the symmetric division probability (rate or percentage) and the cell cycle duration. The rest of the transition probabilities are the same for all executions (see Table I). Each GC has been initialized with 100 proliferating stem cells. All other cell category populations have been set to zero. The code has been executed until 3000 virtual hours. This time has proved sufficient for the initial hypothetical tumor to produce all cell categories and for the relative populations (percentages) of the cell categories to practically reach an equilibrium. It is noted that in real tumors all cell category populations extant at a given (initial) time point except for the stem/clonogenic cells die and subsequently disappear. The latter are the only ones capable of regenerating the tumor on a large time scale. This is depicted in Fig. 5, where three indicative executions characterized by the same cell category transition probabilities and variable cell cycle duration (T_C=30 h, 60 h, 90 h) have been performed.

Table III shows that an increase of the P_{sym} value leads to an increase of the fraction of stem cells in the tumor. This is fairly reasonable since more and more stem cells are produced following consecutive stem cell mitoses. A decrease in the differentiated cell fraction is also evident. This is also expected since less (progenitor) cells can now embark on differentiation. The fraction of limp (progenitor) cells on the other hand exhibits an initial increase, reaches a maximum and then decreases with a relatively small difference between the minimum and maximum values. Limp cells derive from the asymmetric division of stem cells and their population depends on the product of the following two competitive factors: the number of stem cells and the asymmetric division percentage. The combination of these factors leads to the observed behavior of the limp cell fraction in the tumor as a function of the symmetric division percentage. An increase of T_C leads to an increase of stem and limp cell fractions as both cell categories live for a longer interval and a complementary decrease of the differentiated and dead cells. Finally the grey rows of Table III correspond to combinations of the model parameters that lead to non self-conservative tumors i.e. tumors that shrink by themselves and therefore cannot exist [see APPENDIX B].

V. RESULTS

In the following a small number of parametric studies are presented as indicative checks and/or applications of the model. Our primary aim is to deepen and advance quantification of our understanding of tumor response to chemotherapeutic treatment particularly in the breast cancer and more specifically in the TOP trial context.

A homogeneous breast cancer spherical tumor of diameter 14 mm has been considered. The values assigned to the

various input model parameters are included in Table II and III. The various cell category relative populations have been properly initialized using the concept of the nomogram.
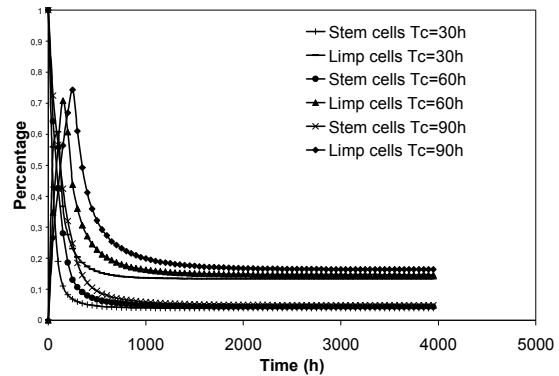
Fig. 5. Fluctuation of stem and progenitor cell population percentages, as functions of time, for three indicative values of the cell cycle duration: 30h, 60h and 90h. The cell category transition probabilities are the same in all three cases. P_{sym}=0.22. The rest of the transition probabilities have been assigned the values included in Table I. The tumor space was initially occupied only by stem cells with a hypothetical (fully artificial) density of 100 cells/mm^3. Each execution corresponds to a tumor with different growth rate. T_C=90h corresponds to the most slowly evolving tumor. It is evident that by 3000 h the population percentages (relative populations) have been stabilized in all cases. The same holds true for the differentiated and dead cell populations (not shown here).

TABLE III
PART OF THE NOMOGRAM OF CELL CATEGORY TRANSITION RATES
(PERCENTAGES) AND CELL CATEGORY RELATIVE POPULATIONS
(FRACTIONS)

Cell cycle duration (h)	Symmetric division percentage	Stem cell fraction	Limp cell fraction	Diff cell fraction	Dead cell fraction
	10%				
	20%	0.032	0.118	0.828	0.022
	30%	0.072	0.190	0.718	0.020
	40%	0.126	0.242	0.612	0.019
30	50%	0.199	0.274	0.508	0.019
	60%	0.295	0.281	0.405	0.019
	70%	0.416	0.262	0.303	0.020
	80%	0.567	0.211	0.201	0.021
	90%	0.751	0.125	0.100	0.024
	10%				
	20%	0.037	0.133	0.810	0.021
	30%	0.075	0.199	0.706	0.020
	40%	0.130	0.248	0.603	0.019
60	50%	0.203	0.278	0.501	0.018
	60%	0.298	0.284	0.400	0.018
	70%	0.419	0.263	0.299	0.019
	80%	0.570	0.212	0.199	0.020
	90%	0.754	0.126	0.099	0.021
	10%				
	20%				
	30%	0.080	0.212	0.688	0.020
	40%	0.135	0.258	0.589	0.019
90	50%	0.208	0.285	0.490	0.018
	60%	0.303	0.289	0.391	0.018
	70%	0.423	0.266	0.293	0.018
	80%	0.574	0.213	0.195	0.018
	90%	0.757	0.126	0.097	0.020

The following three values of the symmetric division fractions (corresponding to the respective percentages) have been considered: 0.19, 0.20 and 0.21. For each case two kinds of executions have been performed; one simulating free tumor growth and another one simulating its response to chemotherapy. Bolus administration of epirubicin is assumed according to the fragmentation scheme shown in Fig. 3. Fig. 6 shows the number of total cells as well as the number of stem and limp cells (both proliferating and dormant). In the case of treatment (therapy) these populations include both surviving cells and cells affected by the drug (and therefore destined to die) but not yet dead.

Although a quantitative validation of the results using actual pseudonymized TOP trial data is in progress, the following observations can already be made based on Fig. 6. In the case of free tumor growth, monotonic growth (actually part of the corresponding Gompertzian curve) has been successfully demonstrated. Depending on the numerical value assigned to the symmetric division fraction both aggressive or slowly progressing tumors can be simulated. More specifically an increase in P_{sym} leads to a tumor with a higher growth rate.

The model also successfully simulates the shrinkage of the tumor after a chemotherapeutic session. The drug administration time points are evident in the corresponding curves as they are accompanied by a rapid decrease in all cell category populations shown. By assigning different values to the various model parameters different clinical cases corresponding e.g. to responding or non responding patients can be simulated. Increasing the value of P_{sym} leads to less pronounced tumor shrinkage following chemotherapeutic treatment as expected.

Numerical findings also indicate that the most appropriate time for tumor removal surgery i.e. the time at which tumor size reaches a minimum depends on the tumor characteristics. More specifically the tumor size seems to be minimum around 38, 30 and 23 days after last drug administration for P_{sym}= 0.19, 0.20 and 0.21 respectively. Until this time the therapeutic effect is still ongoing. Later on the therapeutic benefits may be eliminated due to tumor repopulation. Fig. 7 demonstrates the three dimensional expansion and shrinkage of the tumor. A tumor with P_{sym}=0.19 is depicted 126 days after the beginning of the simulation. Both free growth and response to chemotherapy are considered. The spherical shape of the tumor is practically preserved in both cases. A typical execution time for the simulation of the treatment course on a standard laptop machine is about 2 min. However there is a tremendous increase in the computational power needed with increasing spatial discrimination.

VI. DISCUSSION

Novel approaches to the integrated simulation of a number of crucial aspects of tumour growth and response to therapy have been presented. The first approach is related to the division of potentially proliferating tumor cells to stem/clonogenic cells with theoretically limitless mitotic capacity and progenitor cells with limited mitotic capacity. Such an approach can also implement the theory of stem cell origin of cancer.

According to this theory only a small population of immature (stem) cells is responsible for the generation of a tumor showing resistance to current therapies. These cells are responsible for the regrowth of the tumor even though no tumor is detectable after completion of treatment. A research trend is to produce agents that will target stem cells and eradicate cancer form its root.
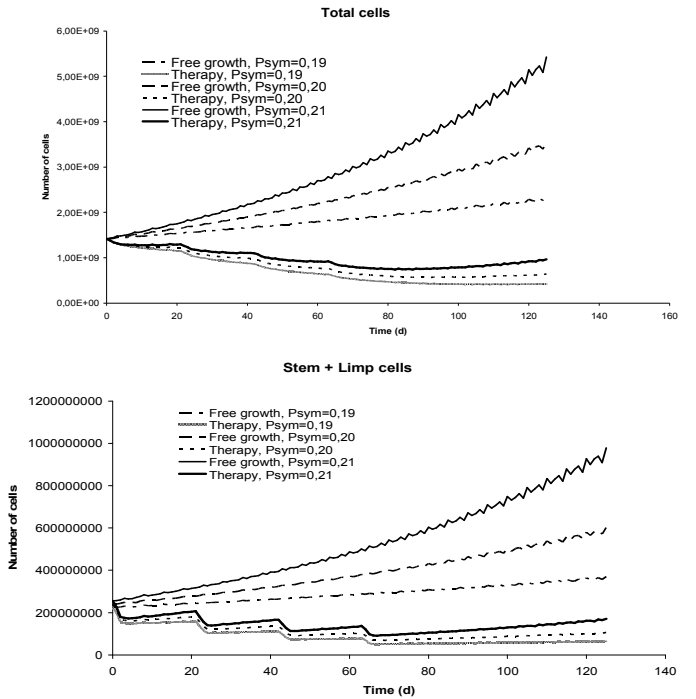
Fig. 6. Number of total tumor cells (Upper Panel) and number of stem and limp (both proliferating and dormant) tumor cells (Lower Panel) as a function of time for the following values of symmetric division fraction P_{sym}: 0.19, 0.20 and 0.21. A homogeneous spherical tumor of diameter equal to 14 mm is considered. Free growth and response to therapy are simulated. Epirubicin is administrated according to the fractionation scheme of Fig. 3. The dose of each fraction is 100mg/m². The values of code input parameters except P_{sym} are included in Table I.
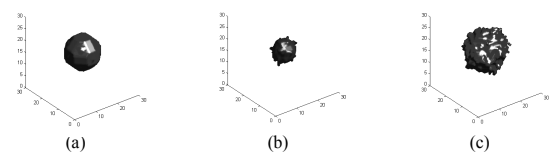
Fig. 7. Three dimensional visualization of a tumor for P_{sym}=0.19. The rest of the values of the model parameters are included in Tables I and II. (a) Initial homogeneous spherical tumor of diameter 14 mm. (b) Tumor at the end of the simulation execution in the case of treatment (126 days after the beginning of chemotherapy and 9 weeks after the last drug administration). The fractionation scheme of Fig. 3 for a fraction dose of 100mg/m² has been considered. (c) Final tumor at the end of the simulation execution in the case of free growth (126 days after the time point corresponding to the start of chemotherapy in panel (b)).

Cancer progenitor cells play an important role in the definition of the tumor grade. In the present version of the model cancer progenitor cells have been considered undergoing three mitoses before they become differentiated. However more progenitor mitotic stages can be supported by the model and this will be demonstrated in future versions. By varying the number of progenitor mitotic stages tumors with different differentiation degrees can be simulated.

Another novel aspect of the model is the concept of the nomogram matching cell category transition rates with cell category relative populations for free tumor growth at the starting point of free tumour growth simulation. Ideally relative populations should be defined for all possible combinations of code parameters values but this is impractical. Subsequent versions of the model will have incorporated the estimation of the cell category relative populations in the main code module and therefore they will substantially increase usability of the code.

The model developed aims to intensively exploit the individual patient's medical data such as imaging data (e.g., CT, MRI, PET slices, possibly fused), histopathological data (e.g., tumor subtype, differentiation degree etc.), molecular data (e.g. critical gene expressions) and clinical data (age, previous treatments etc.). Extensive demonstrations of these processes, already implemented within the framework of ACGT, will be presented shortly.

A small number of parametric studies have also been presented. Similar studies are to be performed for all code parameters in order to thoroughly analyse the sensitivity of the model's behavior to its parameters variations. An extensive use of the clinical trial data is expected to crucially support the model's optimization and clinical adaptation. Pertinent optimization techniques such as artificial neural networks, genetic algorithms etc. have been planned to be used in this context.

Based on the results obtained so far as well as on their critical analysis the simulation model appears to be capable to satisfactorily simulate, at least qualitatively, many clinically important features of tumor behavior such as tumor repopulation, expansion and shrinkage.

VII. CONCLUSIONS

A top-down four-dimensional multilevel Monte Carlo discrete state simulation model of the response of solid tumors such as breast cancer tumors to epirubicin-based chemotherapeutic treatment *in vivo* has been presented. Special emphasis has been put on the effect of the stem/clonogenic, progenitor, differentiated and dead cells on the overall tumor behavior. The importance of adaptation of the cell category relative populations to the cell category transition rates for free cell growth has been revealed and the concept of a pertinent nomogram has been introduced. A method which ensures adaptation of these two sets of entities at the beginning of the simulation execution has been proposed and applied. A preliminary parametric study has

been performed and a number of interdependences have been revealed. Although a thorough numerical analysis of the model in order to accurately determine its sensitivity and parameter interdependences is under way, results obtained so far are in agreement with clinical reality. A thorough clinical validation and optimization by exploiting pseudoanonymized real data from the TOP trial within the framework of the ACGT project is in process. Our goal is to end up with a reliable simulation system able to assist clinicians with personalized optimization of cancer treatment. Optimization is expected to be achieved through performing *in silico* (on the computer) patient individualized treatment experiments. The clinically validated model might also serve as a valuable tool for researchers, professionals or patients.

APPENDIX A

For a three-compartment first order pharmacokinetic model the plasma drug concentration can be given by:

$$C = A\mathrm{e}^{-at} + B\mathrm{e}^{-\beta t} + \varGamma\mathrm{e}^{-\gamma t} \qquad (2)$$

The Area Under Curve is

$$AUC = \frac{A}{a} + \frac{B}{\beta} + \frac{\varGamma}{\gamma} \qquad (3)$$
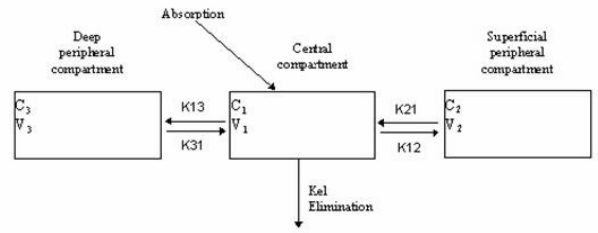
Fig. 8. Three compartment model. Ci, Vi are the concentration and volume of each compartment, kel is the elimination rate constant from the central compartment, and k12, k21, k13, k31 are the rate constants describing drug transfer between the compartments.

where

$$a = k_{el} + k_{12} + k_{21} + k_{13} + k_{31}., c = k_{el} \cdot k_{21} \cdot k_{31}$$

$$b = k_{el} \cdot k_{21} + k_{el} \cdot k_{31} + k_{12} \cdot k_{31} + k_{31} \cdot k_{21} + k_{21} \cdot k_{13}$$

$$\phi = \arctan \sqrt{\frac{\left(\left(\frac{a}{3}\right)^2 - \frac{b}{3}\right)^3}{\left(\left(\frac{a}{3}\right)^3 + \frac{c - \frac{a*b}{3}}{2}\right)} - 1},$$

$$\alpha = \frac{a}{3} + 2 * \sqrt{\left(\frac{a}{3}\right)^2 - \frac{b}{3}} * \cos(\frac{\phi}{3}),$$

$$\beta = \frac{a}{3} + 2 * \sqrt{\left(\frac{a}{3}\right)^2 - \frac{b}{3}} * \cos(\frac{\phi}{3} + \frac{4 \cdot \pi}{3}),$$

$$\gamma = \frac{a}{3} + 2 * \sqrt{\left(\frac{a}{3}\right)^2 - \frac{b}{3}} * \cos(\frac{\phi}{3} + \frac{2 * \pi}{3}),$$

$$A = \frac{D}{V_1} \frac{(\alpha - k_{21}) \cdot (\alpha - k_{31})}{(\alpha - \beta) \cdot (\alpha - \gamma)}, B = \frac{D}{V_1} \frac{(\beta - k_{21}) \cdot (\beta - k_{31})}{(\beta - \alpha) \cdot (\gamma - \alpha)}$$

$$\Gamma = \frac{D}{V_1} \frac{(\gamma - k_{21}) \cdot (\gamma - k_{31})}{(\gamma - \beta) \cdot (\gamma - \alpha)}$$

APPENDIX B

Let us consider N stem cells residing in the G1 cell cycle phase. After each execution step (every hour) a fraction of stem cells will die due to apoptosis. This procedure is quantified by the parameter *apoptosis rate* (R_A). More specifically after the first hour a number of $N(1- R_A)$ cells will remain alive, after the second the stem population will be $N(1- R_A)^2$ etc. The number of stem cells that will eventually reach the mitosis phase and subsequently divide will be $N(1-R_A)^{T_C}$. From this population a fraction equal to P_{sym} will divide symmetrically giving rise to 2 stem cells, whereas the rest of the stem cells will give birth to 1 stem cell and 1 progenitor cell. By performing the necessary computations the number of stem cells after mitosis will be $N(1-R_A)^{T_C}(1+P_{sym})$. The stem cells that will re-enter the cell cycle and will not enter the dormant (G0) phase will be $N(1-R_A)^{T_C}(1+P_{sym})(1-P_{MtoG0})$. In order to have a growing tumor the number of stem cells after mitosis must be larger than the number of the initial stem cells i.e the following inequality must hold true

$$N(1-R_A)^{T_C}(1+P_{sym})(1-P_{MtoG0}) \geq N \Rightarrow$$

$$(1-R_A)^{T_C}(1+P_{sym})(1-P_{MtoG0}) \geq 1 \qquad (4)$$

Equation (4) enables computation of the allowed value range of any one of the parameters, for example P_{sym}, provided that specific values have been assigned to the trest of the parameters. In the above analysis the fraction of dormant cells that re-enter the cell cycle (expressed by P_{G0toG1}) has not been taken into account. Nevertheless for low values of P_{G0toG1} as is the case of free tumor growth (4) is a good approximation.

REFERENCES

[1] World Health Organization International Agency for Research on Cancer (June 2003). World Cancer Report. Retrieved on 2008-06-17.

[2] B Fisher, J Bryant, N Wolmark, E Mamounas, A Brown, ER Fisher, DL Wickerham, M Begovic, A DeCillis, A Robidoux, RG Margolese, AB Cruz Jr, JL Hoehn, AW Lees, NV Dimitrov and HD Bear, "Effect of preoperative chemotherapy on the outcome of women with operable breast cancer," *J. Clin. Oncol.,* vol. 16, pp. 2672-85, 1998.

[3] S. Chuang, "Mathematic models for cancer chemotherapy: pharmacokinetic and cell kinetic considerations," *Cancer Chemother. Rep.,*vol. 59, no. 4, pp. 827–42, 1975.

[4] S. Ozawa, Y. Sugiyama, J. Mitsuhashi, and M. Inaba, "Kinetic analysis of cell killing effect induced by cytosine arabinoside and cisplatin in relation to cell cycle phase specificity in human colon cancer and chinese hamster cells," *Cancer Res.*, vol. 49, pp. 3823–3828, 1989.

[5] S. N. Gardner, "Modeling multi-drug chemotherapy: Tailoring treatment to individuals*," J. Theor. Biol.*, vol. 214, pp. 181–207, 2002.

[6] V. Durbecq, M. Paesmans, F. Cardoso, C. Desmedt, A. Di Leo, S. Chan, K. Friedrichs, T. Pinter, S. Van Belle, E. Murray, I. Bodrogi, E. Walpole, B. Lesperance, S. Korec, J. Crown,11 P. Simmonds, T. J. Perren, J.-Y. Leroy, G. Rouas, C. Sotiriou, M. Piccart, and D. Larsimont, "Topoisomerase-IIA expression as a predictive marker in a population of advanced breast cancer patients randomly treated either with single-agent doxorubicin or single-agent docetaxel*," Mol Cancer Ther*, vol. 3, pp. 1207-1214, October 2004

[7] G.S. Stamatakos, D.D. Dionysiou, E.I. Zacharaki, N.A. Mouravliansky, K.S.Nikita, N.K. & Uzunoglu , In silico radiation oncology: combining novel simulation algorithms with current visualization techniques , IEEE Proceedings: Special Issue on Bioinformatics: Advances and Chalenges , 90(11) , 1764-1777 , 2002.

[8] D. D. Dionysiou, G. S. Stamatakos, N.K. Uzunoglu, K. S. Nikita, A. Marioli, "A four-dimensional simulation model of tumour response to radiotherapy in vivo: parametric validation considering radiosensitivity, genetic profile and fractionation,"Journal of Theoretical Biology vol. 230, pp. 1–20, 2004

[9] G. S. Stamatakos, V. P. Antipas and N. K. Uzunoglu, "A Spatiotemporal, Patient Individualized Simulation Model of Solid Tumor Response to Chemotherapy in Vivo: The Paradigm of Glioblastoma Multiforme Treated by Temozolomide," *IEEE Transactions On Biomedical Engineering*, vol. 53, pp. 1467- 1477, August 2006

[10] G.S.Stamatakos, D.D.Dionysiou, N.M.Graf, N.A.Sofra, C.Desmedt, A.Hoppe, N.Uzunoglu, M.Tsiknakis , "The Oncosimulator: a multilevel, clinically oriented simulation system of tumor growth and organism response to therapeutic schemes. Towards the clinical evaluation of in silico oncology," Proceedings of the 29th Annual International Conference of the IEEE EMBS Cite Internationale, August 23-26, SuB07.1: 6628-6631 , Lyon, France , 2007

[11] G. Steel, Basic Clinical Radiobiology. Arnold, London, UK. 2002.

[12] S.E.Salmon and A.C.Sartorelli "Cancer Chemotherapy", in Basic & Clinical Pharmacology, B.G.Katzung, ed. Lange Medical Books/McGraw-Hill, International Edition, pp.923-1044, 2001.

[13] R.Danesi, F.Innocenti, S.Fogli, A.Gennari, E.Baldini, A.Di Paolo, B.Salvadori, G.Bocci, P.F.Conte and M.Del Tacca, "Pharmacokinetics and pharmacodynamics of combination chemotherapy with paclitaxel and epirubicin in breast cancer patients", *Journal of Clinical Pharmacology*, vol. 53, pp 508-518, 2002.

[14] http://depts.washington.edu/saam2/

[15] M.C.Perry ed. The Chemotherapy Source Book. USA, Philadelphia: Lippincott Williams &Wilkins, 2008.

[16] http://www.fda.gov/cder/foi/nda/99/50-778_Ellence_pharmr.pdf

[17] J.Lankelma, H.Dekker, R.F. Luque, S.Luykx, K.Hoekman, P.van der Valk, P.J.van Diest, H.M.Pinedo, " Doxorubicin gradients in human breast cancer," *Clin Cancer Res*, vol. 5, pp. 1703-1707, 1999.